Pergamon

Geochimica et Cosmochimica Acta, Vol. 66, No. 23, pp. 4149–4163, 2002

0016-7037/02 $22.00 + .00

PII S0016-7037(02)01000-1

Water dissolution in albite melts: Constraints from *ab initio* NMR calculations

YUN LIU, HANNA NEKVASIL,* and HONGBO LONG

Department of Geosciences, State University of New York at Stony Brook, NY, 11794-2100, USA

(*Received March* 4, 2002; *accepted in revised form June* 17, 2002)

Abstract—Hartree-Fock and B3LYP NMR calculations were performed at the 6–311+G(2df,p) level on cluster models representing albite glasses using B3LYP/6 to 31G* optimized geometries. Calculation results on several well-known crystalline materials, such as low albite and $KHSi_2O_5$, were used to check the accuracy of the calculation methods.

Calculated ^{29}Si-NMR results on clusters that model protonation of Al-O-Si linkages and the replacement of Na^+ by H^+ indicate a major increase in Si-O(H) bond length and a 5 ppm difference in δ_{iso} for ^{29}Si compared to that for anhydrous albite glass. The calculated δ_{iso} of ^{27}Al in such linkages agrees with the experimental data, but shows an increase in C_q that cannot be fully diminished by H-bonding to additional water molecules. This protonation model is consistent with both experimental ^{17}O NMR data and the major peak of ^{1}H-NMR spectra. It cannot readily explain the existence of the small peak in the experimental ^{1}H spectra around 1.5 ppm. Production of the depolymerized units Al [Q^3]-O-H upon the dissolution of water is not consistent with ^{27}Al, ^{1}H, or ^{17}O NMR experimental results. Production of Si [Q^3]-O-H is consistent with all of the experimental ^{17}O and ^{1}H-NMR data; such units can produce both the major peak at 3.5 ppm and the small peak at 1.5 ppm in ^{1}H spectra, either with or without hydrogen bonding. This species, however, cannot produce the main features of ^{29}Si spectra.

It is concluded that although neither protonation nor the production of Si [Q^3]-O-H alone is consistent with the available experimental data, the *combination* of these two processes is consistent with available experimental NMR data.

1. INTRODUCTION

Many properties of igneous systems, from viscosity and density, to electrical conductivity and mineral/melt equilibria, are strongly affected by dissolved water (e.g., Burnham, 1975; Lange, 1994; Hess and Dingwell, 1996; Dingwell, 1998). In view of the link between the microscopic state and macroscopic properties, understanding these varied effects requires a detailed understanding of the water dissolution mechanism.

Using hydrous glasses as a proxy for liquids, it has been shown from early spectroscopic studies that water dissolution in aluminosilicate melts produces two readily distinguishable groups: H_2O molecules and hydroxyl groups (e.g., Stolper, 1982; Mysen and Virgo, 1986; Silver and Stolper, 1989; Withers and Behrens, 1999). It remains well accepted that at low water contents (i.e., less than a few percent), hydroxyl (-OH) groups dominate. With increasing water content, however, the proportion of structurally-bound molecular water in the glass increases markedly (e.g., Silver and Stolper, 1989; Richet and Polian, 1998; Mysen and Wheeler, 2000; Schmidt et al., 2001a).

It has also been recognized that through the production of terminal hydroxyls, water can depolymerize the network of Al-free silicate melts (e.g., SiO_2 glass, Farnan et al., 1987 sodium silicate glass, Kummerlen et al., 1992) and form (O-)$_3$Si-O-H linkages (referred to from here on as Si[Q^3]-O-H). But whether or not water dissolution in alkali aluminosilicates glasses, such as albite, also induces depolymerization is still debated.

Based on NMR experimental data, Kohn et al. (1989), Kohn et al. (1992), Kohn et al. (1994) and Kohn et al. (1998) concluded that there is no evidence for depolymerization of the albite glass framework by rupture of T-O-T linkages as in silica; rather, a $Na^+ \leftrightarrow H^+$ cation exchange occurs which leads to the formation of bridging hydroxyl groups (Al-O(H)-Si) and an equal number of Na^+OH^- complexes. Their conclusion was based on the similarity of ^{27}Al and ^{29}Si-NMR spectra for dry and hydrous albite glasses and the dramatic change of ^{23}Na spectra with increasing water content. Furthermore, little difference was observed between ^{17}O NMR spectra of dry and hydrous glass (e.g., Xu et al., 1998; Maekawa et al., 1998). From ab initio GIAO (Gauge-Independant Atomic Orbital) NMR calculations, however, Sykes et al. (1997) concluded that both the calculated Al isotropic chemical shift and Al QCCs (quadrupolar coupling constants) for the structures proposed by Kohn et al. (1989) were not consistent with experimental results. More recently, Tossell (1999) found that the calculated ^{23}Na NMR trend for the model proposed by Kohn et al. (1989) will be different that what was observed and suggested that Na^+ may not be fully replaced by H^+ but rather has some O-containing ligands in its coordination sphere.

Sykes and Kubicki (1993, 1994) suggested, based on infrared and Raman spectroscopy and quantum chemistry calculations, that water dissolves in aluminosilicate melts through the formation of Al and Si hydroxyls by breaking Al-O-Al or Al-O-Si linkages. This is consistent with the early explanation of the macroscopic changes in melt properties offered by Burnham (1975). However, Dirken et al. (1997) found no detectable Al-O-Al in ^{17}O MQ-NMR (Multiple-Quantum NMR) spectra of albite glass. Although this does not disprove depolymerization, it does suggest that depolymerization based on reaction

* Author to whom correspondence should be addressed (Hanna.Nekvasil@sunysb.edu).

with Al-O-Al is not likely the primary mechanism of water dissolution. Focusing on the Al-O-Si units, Zeng et al. (1999, 2000) indicated that their TRAPDOR NMR data were consistent with the formation of Al [Q^3]-O-H and Si [Q^3]-O-H upon dissolution of H_2O into aluminosilicate glasses, as well as possible cation exchange between H^+ and Na^+.

The ^{1}H-^{29}Si CPMAS NMR results of Oglesby and Stebbins (2000) fit both water dissolution models but also indicated the possibility of a large amount of SiOH or protonated bridging O atoms in hydrated glasses. Oglesby et al. (2001) investigated the ^{17}O NMR properties of crystalline potassium hydrogen disilicate ($KHSi_2O_5$) and compared the results with glasses of hydrous potassium silicate, hydrous potassium aluminosilicates, and hydrous haplogranite compositions. They found that hydrous potassium silicate glass contained Si-OH species similar to those in $KHSi_2O_5$, but these species were not evident in the hydrous potassium aluminosilicate or haplogranite glasses. These results are most consistent with the conclusions of Kohn et al. (1989) if the Si-OH(Na^+) environment is not much different from that of Si-OH(K^+). Further ^{17}O NMR experimentation suggested significant interactions between cations (i.e., Ca^{2+}, K^+, Na^+) and molecular H_2O in hydrous aluminosilicate glasses (Oglesby et al., 2002). Schmidt et al. (2001b) investigated the effects of hydration on two series of aluminosilicate glasses with $Ab_{39}Or_{32}Qz_{29}$ and $Qz_{37}Ab_{63}$-$Qz_{34}Or_{66}$ compositions. Although their results were generally consistent with the model of Kohn et al. (1989), the ^{1}H-NMR data indicated the presence of more than one type of OH-bearing group, suggesting the possibility of more than one dissolution mechanism and the possible presence of Al-OH. Further calculations made by Kubicki and Sykes (2001) concluded that Al-OH species are not likely to be abundant. Instead, they concluded that the Si-(OH) and T-(OH)-T species were most consistent with the current NMR data on hydrous albite glass.

It is clear that NMR experimentation has strong potential for providing exciting new insights into water dissolution mechanisms. Yet, the interpretation of experimental NMR results on glasses can be ambiguous. This work aims to help constrain the interpretation of NMR data on hydrous glasses by using ab initio calculations on cluster models carefully selected to model possible water dissolution products. Both Hartree-Fock and hybrid DFT (density functional theory) (i.e., B3LYP) calculations were performed on all clusters. The uncertainty ranges of the results on different nuclei using different methods have also been carefully evaluated.

2. CALCULATION METHODS

2.1. Geometry Optimization

All the calculations have been performed by using GAUSSIAN 98 (Frisch et al., 1998). Geometry optimizations used the B3LYP DFT (density functional theory) method (with Becke's three-parameter hybrid functional using the LYP correlation functional, Lee et al., 1988; Becke, 1993). The chosen basis set was the standard polarized split-valence 6 to 31G*, because the geometry results of 6 to 31G* often have an accuracy equivalent to that of much larger basis sets (Foresman and Frisch, 1996).

2.2. NMR Calculations

NMR shielding tensor calculations were performed using the gauge-independent atomic orbital (**GIAO**) method (the ab initio version first published by Ditchfield, 1974). It computes chemical shieldings for nuclei based on coupled perturbation theory that involves solving for the second derivative of the energy with respect to the magnetic field and the magnetic moment of the nucleus.

Using the GIAO formalism, the isotropic shielding σ_{iso} is obtained by averaging the three principal tensor components, σ_{xx}, σ_{yy} and σ_{zz} of the 3×3 tensor matrix. Isotropic chemical shifts δ_{iso} were calculated using the relationship $\delta_{iso} = \sigma_{iso}^{ref} - \sigma_{iso}^{molecule}$, where σ_{iso}^{ref} is the chemical shielding value of a reference substance [TMS chosen here for ^{29}Si and ^{1}H; Al^{3+}•6(H_2O) for ^{27}Al; liquid water for ^{17}O] calculated at the same level. Nuclei with a nuclear spin quantum number of $I > 1$, (e.g., ^{27}Al) will have nonspherical nuclear charge distributions and hence an electric quadrupolar moment Q. For such cases, the experimental peak will be

$$\delta_{peak} = \delta_{iso} - \delta_{qs} \tag{1}$$

where δ_{peak} is the observed peak, δ_{iso} the isotropic chemical shift, and δ_{qs} the second order quadrupolar shift. If there is no available isotropic chemical shift data from experiments, the δ_{qs} is needed to compare the calculation results directly against experimental spectra. It can be calculated from the equation

$$\delta_{qs} = -\frac{3\,C_q^2}{40\,\nu_L^2}\frac{I(I+1) - 9m(m-1) - 3}{I^2(2I-1)^2}\left(1 + \frac{\eta^2}{3}\right) \tag{2}$$

where ν_L is the Larmor frequency, I is the nuclear spin quantum number, and m is the magnetic spin quantum number. The C_q (quadrupolar coupling constant) $= e^2Qq$, and consists of the nuclear quadrupolar moment Q, the electric field gradient q, and the fundamental constant e. The asymmetry parameter $\eta = |(q_{xx} - q_{yy})/q_{zz}|$, where q_{xx}, q_{yy} and q_{zz} are the principal tensor components of the electric field gradient (EFG).

3. FURTHER CONSIDERATIONS

3.1. Calculation Levels

Basis set size. Although the GIAO method has the advantage of faster convergence for different sizes of basis sets, we chose the 6-311+G(2df,p) for all NMR calculations.

^{29}Si-NMR. The Hartree-Fock level was found to be sufficiently accurate for ^{29}Si–NMR calculations. There are many examples for which the calculated HF level results are in excellent quantitative agreement with the experimental ones (e.g., for zeolites, Bull et al., 2000; silica glass, Sykes et al., 1997). Hence, the HF/6-311+G(2df,p) level was used to calculate all ^{29}Si-NMR properties in this paper.

^{27}Al NMR. Our calculations have occasionally indicated a several ppm difference between the calculated chemical shift using the Hartree-Fock and the B3LYP DFT methods. The Hartree-Fock theorem does not take into account any electron correlation effects. In contrast, the B3LYP method includes an electron correlation treatment by using a parameterized exchange potential, but often overestimates it. For

the ^{27}Al NMR calculations, it is difficult to assess which method is better. We list the results of both levels but believe that the *average* value of HF and B3LYP for ^{27}Al NMR may be closer to the real value.

As discussed in Liu and Nekvasil (2001), the EFG calculation is not trustworthy when using small clusters that include cations (since the electric field gradient decays slowly as 1/r). Because we have included Na^+ ions in the cluster models considered here, we discuss primarily the trend of the C_q. For quadrupolar shift calculation, we use either an experimental C_q value or discuss only the isotropic chemical shift (δ_{iso}) of ^{27}Al.

^{17}O NMR. Commonly, oxygen atoms in silicates contain two electron lone pairs. This results in significant electron correlation effects. Because it lacks any treatment of electron correlation effects, again, the Hartree-Fock level has a poor performance record for yielding ^{17}O NMR parameters. A DFT method, such as B3LYP, is better but still, its precision is questionable (e.g., Wilson et al., 1999). Unfortunately, higher level methods such as MP2 (Moller Plesset perturbation method of second order) and CCSD (coupled cluster method) are impractical for even slightly larger model clusters. In practice, we have used the B3LYP/6 to 311+G(2df,p) level to calculate ^{17}O NMR parameters and acknowledge the possibility of a several ppm uncertainty. The accuracy of this level is further discussed below through comparisons of calculations on well-known crystalline materials such as albite and $KHSi_2O_5$.

Like ^{27}Al,^{17}O is also a nucleus with quadrupolar moment. Fortunately, its nuclear quadrupolar moment *Q* is much smaller than that for ^{27}Al. Nonetheless, here we also use the experimental ^{17}O C_q values, or only discuss ^{17}O's isotropic chemical shifts. To aid in the calculation of ^{17}O NMR parameters, we used oxygen-centered clusters instead of the more common Si- or Al- centered clusters.

^{1}H NMR. There are only small differences (<1 ppm) between the HF and B3LYP results for ^{1}H. We used the B3LYP/6 6–311+G(2df,p) level for the calculations discussed below

3.2. The ^{17}O Reference

Water at room temperature is commonly used as a reference for ^{17}O NMR experiments. Therefore, to calculate the ^{17}O chemical shift of albite glass, that of liquid water must also be calculated. This necessitates a choice of model representing liquid water. Xue and Kanzaki (2000, 2001) and Tossell (2001) used the gas-phase H_2O molecule itself and ignored the gas-liquid 36 ppm shielding shift. Kubicki and Sykes (2001) and Kubicki and Toplis (2002) used a cluster with 19 H_2O molecules to represent liquid water and obtained a gas-to-liquid shift of 41 ppm. Both of these choices may be less than ideal. Structurally, liquid water will certainly differ from monomeric H_2O (e.g., Cq varies between water phases). However, a cluster model built from a large number of arbitrarily placed water molecules can easily produce some strong ice-like linkages during the free optimization for the energy minimum. Hence, the choice of a model for liquid water is not straightforward and requires further consideration.

It is well accepted that liquid water has a cyclic structure (i.e., Estrin et al., 1996; Xantheas and Dunning, 1993). Some theoretical results, such those based on the quantum cluster equilibrium (QCE) theory, suggest that liquid water consists mainly of 2 to 3-coordinate ring clusters (Ludwig and Weinhold, 1999) (where "*n*-coordinate" refers to the number n of hydrogen bonds that each water molecule forms with other water molecules). These rings are restricted to a rather small size (e.g., 5 or 6 water molecules). Using, in addition, the experimental constraints of the gas to liquid ^{17}O NMR chemical shift difference for water (36 ppm; Florin and Alei, 1967; Nymand et al., 1997) and the average O. . .H hydrogen bond distance (1.85Å; e.g., Thiessen and Narten, 1982), we have tried to use several cyclic water clusters to calculate the ^{17}O isotropic shift.

First, we tested the strong 2-coordinate situation by using the 5- or 6-membered rings shown in Figures 1a and b. This produces a 30 ppm "gas-to-liquid" shift ($\Delta\delta$). However, these gas phase rings are not like those in liquid water since the O. . .H hydrogen bond distance is 1.70 Å. In liquid water, interactions from the surrounding environment (i.e., weak hydrogen bonding) will make these 2-coordinate rings larger. We have tested the possibility of larger rings by using a more relaxed 6-membered ring of water molecules but fixing all O. . .H at 1.85 Å. In addition, we added another two water molecules to this 6-membered ring to represent further interactions (see Fig. 1c). To prevent these two H_2O molecules (labeled 1 and 2 in Fig. 1c) from becoming immediately attached to the ring, we gave them slightly longer O. . .H hydrogen bond distances (2.0 Å) within the ring. The two O atoms in the 6-membered ring (labeled A and B in Fig. 1c) now yield a 27 ppm "gas-to-liquid" shift. Thus, it appears that two strong hydrogen bonds yield almost the same "gas-to-liquid" shift as three weak hydrogen bonds. We also tested the strong 3-coordinate configurations of Figures 1d and e. The more "relaxed" 3-coordinate configuration has a "gas-to-liquid" shift of 40 ppm, while the ice-like configuration has one of 45 ppm. The strong, ice-like, 4-coordinate configuration (Fig. 1f) yields a $\Delta\delta$ of 64 ppm.

The peak at maximum position in the experimental ^{17}O NMR spectrum of water has a "gas-to-liquid" $\Delta\sigma$ of 36 ppm. We believe the gas-to-liquid shift to be somewhere between the values of the 2-coordinate and 3-coordinate configurations rather than at that of the ice-like one. The average lies in the range 34 to 36 ppm, which is very close to the experimental 36 ppm gas-to-liquid shift. We have chosen here to use 286 ppm as the shielding value of water at the B3LYP/6–311+G(2df,p) level which has a "gas-to-liquid" shift of 35 ppm. It is expected that this value has a few ppm uncertainty.

3.3. A Cluster Model for Albite Glass

The albite glass structure is more "relaxed" than its crystalline counterpart. This implies that instead of the predominance of 4-membered rings as in the crystalline structure, glass may contain a variety of rings with a larger number of members (e.g., 6-membered rings, Taylor and Brown, 1979). Such rings would have slightly larger average T-O-T bond angles and each T would show increased shielding. This may explain why the experimental ^{27}Al δ_{iso} for crystalline low albite differs by several ppm from that in albite glass (see Table 1). This difference for Si is small, perhaps because the original Si-O-Si

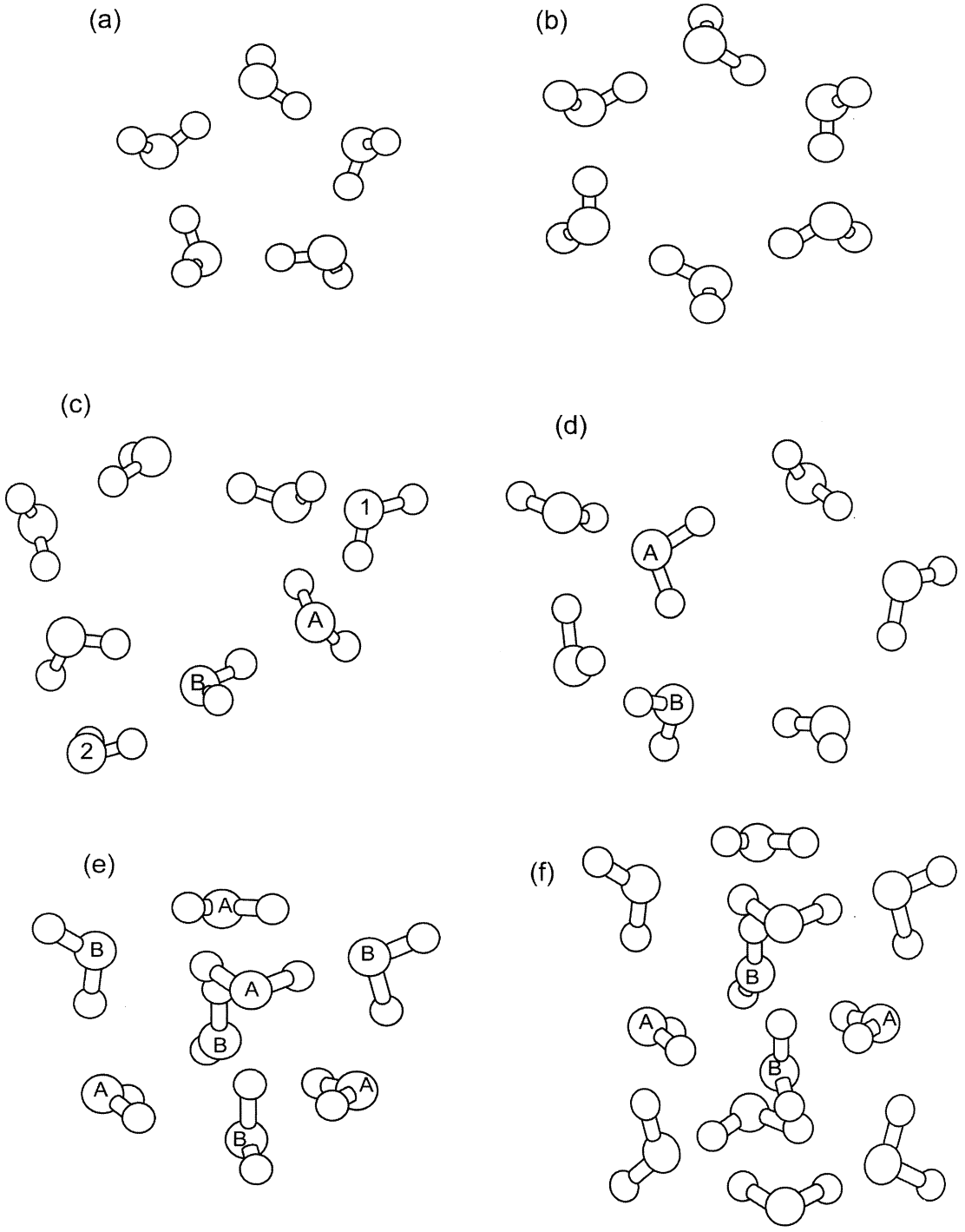

Fig. 1. Clusters used to represent liquid water: (a) 5-membered ring [^{17}O shielding (σ) = 290.3 ppm; shielding difference from gaseous H_2O at same computational level ($\Delta\sigma$) = σ_{H2O} - σ =30.3 ppm], (b) 6-membered ring [σ = 290.6 ppm, $\Delta\sigma$= 30.0 ppm], (c) weak 3-coordinate configuration [σ_A = 291 ppm, σ_B = 295 ppm; average $\Delta\sigma$= 27 ppm], (d) relaxed strong 3-coordinate configuration σ_A = 280.6 ppm, σ_B = 280.7 ppm; average $\Delta\sigma$= 40 ppm], (e) ice-like strong 3-coordinate configuration [σ_A = 272.1 ppm, σ_B = 278.8 ppm; average $\Delta\sigma$= 45 ppm], (f) ice-like strong 4-coordinate structure [σ_A = 256.0 ppm, σ_B = 257 ppm; average $\Delta\sigma$= 64 ppm].

bond angles (in 4-member rings) are already rather large (i.e., 130°, 151° and 161° in low albite, with an average of 147.3°) and further enlargement is difficult. The smaller Al-O-Si bond angles leave more room for enlargement.

Based on such considerations, an albite glass cluster model was constructed which contains a single 4-membered ring and primarily open linkages that represent larger rings. This model can consistently reproduce the observation that nuclei in albite

Table 1. Calculated isotropic chemical shift (δ_{iso}) of ^{29}Si, ^{27}Al, ^{1}H and ^{17}O for the clusters used in this study (in ppm).

		^{29}Si		^{27}Al		^{1}H		^{17}O	
Phase	Linkage (site calculated in boldface)	Calc	Expt	Calc	Expt	Calc	Expt	Calc	Expt
Crystalline low albite	**Si**[Q^4(3Si, 1Al)]$_{T2O}$-**O-Al**[Q^4(4Si,0Al)] Fig. 2a	−96	−96.8[a]	78(?)	63[a]	—	—	41	~33–43[b]
	Si[Q^4(3Si, 1Al)]$_{T2O}$-**O**-Si[Q^4(2Si,2Al)]$_{T2m}$ Fig. 2b	−94	−96.8[a]	—	—	—	—	53	~49–58[b]
	Si[Q^4(3Si, 1Al)]$_{T2O}$-O-**Si**[Q^4(2Si,2Al)]$_{T2m}$ Fig. 2b	−92	−92.3[a]	—	—	—	—		
Crystalline $KHSi_2O_5$	O in SiOH (NBO site) (Fig. 5a)	−98	−97.2[c]	—	—	17.7	—	70	60[d]
	O in SiOSi (BO site) (Fig. 5b)	−91	—	—	—	—	—	51	51[d]
Anhydrous albite glass	**Si**[Q^4(4Si,0Al)]-**O**-Si[Q^4(4Si,0Al)]	−111	—	—	—	—	—	—	—
	Si[Q^4(3Si,1Al)]-**O-Al**[Q^4(4Si,0Al)] Fig. 2c	−98	−98[e]*	61	60[f]*	—	—	41	~33–43[c]
	Si[Q^4(1Si,3Al)]-**O-Al**[Q^4(4Si,0Al)] Fig. 2d	−93	−98[e]*	64	60[f]*	—	—	46	~33–43[c]
Hydrous albite glass									
(1) Protonation model	**Si**[Q^4(3Si, 1Al)]-**O(H)-Al**[Q^4(4Si,0Al)] Fig. 3a	−104	−98[e]*	63	60[f]*	3.6	3.2→[g]*	34	~33–43[c]
	Si[Q^4(2Si,2Al)]-**O(H)-Al**[Q^4(4Si,0Al)] Fig. 3b	−96	−98[e]*	61	60[f]*	12	3.2→[g]*	56	~33–43[c]
	Si[Q^4(3Si,1Al)]-**O(H)**(H_2O)-**Al**[Q^4(4Si,0Al)] Fig. 3c	−103	−98[e]*	64	60[f]*	3.6→	3.2→[g]*	36→	~33–43[c]
(2) Depolymerization model	**Si**[Q^3(3Si,0Al)]-**O-H** Fig. 4a	−101	−98[e]*	—	—	1.5	3.2→[g]*	17	>15[h]
	Si[Q^3(3Si,0Al)]-**O-H** Fig. 4b	−96	−98[e]*	—	—	1.5	3.2→[g]*	20	>15[h]
	Si[Q^3(3Si,0Al)]-**O-H**(H_2O) (at variable O...H_2O distances) (Fig. 4c)	−96 to −103	−98[e]*	—	—	3–8	3.2→[g]*	20–28	>15[h]
	Si[Q^3(2Si,1Al)]-**O-H** Fig. 4d	−84	−98[e]*			6	3.2→[g]*	26	>15[h]
	Si[Q^3(2Si,1Al)]-O-**Al**[Q^4(4Si,0Al)] Fig. 4d			66	60[f]*				
	Al[Q^3(3Si,0Al)]-**O-H** Fig. 4b (with central Al atom)	—	—	73	60[f]*	−1.4	3.2→[g]*	−23	>15[h]
	Al[Q^3(3Si,0Al)]-**O-H**(H_2O) (with 1.8 Å O..H_2O dist)			~70	60[f]*	2.6	3.2→[g]*	−2	>15[h]

Symbols: a: Kirkpatrick (1988); b: Kubicki and Sykes (2001); c: Oglesby and Stebbins (2000); d: Oglesby et al (2001); e: Kohn et al. (1989); f: Schmidt et al. (2000); g: Schmidt et al. (2001a,b); h: based on minimum ^{17}O δ_{iso} value of 15 ppm (Maekawa et al. 1998); * maximum position for broad peak.

glass all have slightly larger shieldings (and smaller δ_{iso}) than their crystalline counterparts (see Table 1).

4. RESULTS AND DISCUSSIONS

4.1. ^{29}Si NMR

Before we interpret the ^{29}Si-NMR results for the glasses, we must first check how accurately we can calculate the ^{29}Si-NMR peak positions for crystalline low albite. Albite has three peaks in its ^{29}Si-NMR spectrum, at −92.3 ppm (T_2m), −96.8 ppm (T_2O) and at −104.3 ppm (T_1m) (e.g., Kirkpatrick, 1988). We calculated the ^{29}Si-NMR properties of a Si[Q^4(3Si,1Al)]$_{T2O}$-O-Al[Q^4(4Si,0Al)] linkage in a fragment of the low albite crystalline structure (where the notation Si[Q^4(3Si,1Al)] refers to a central silicon tetrahedron with four linkages to other tetrahedra, three of which are to other silica tetrahedra and one to an aluminum tetrahedron) containing the T_2O site with a geometry based on X-ray coordinates (Fig. 2a). The T_2O Si site has only one Al in its neighborhood and the Si-O-Al is 139.6°. Its calculated ^{29}Si δ_{iso} is −96 ppm (Table 1), in excellent agreement with the experimental result of −96.8 ppm.

Figure 2b shows a cluster model of a fragment of crystalline low albite containing a Si[Q^4(3Si,1Al)]$_{T2O}$-O-Si[Q^4(2Si,2Al)]$_{T2m}$ linkage, also based on X-ray coordinates. The calculated ^{29}Si δ_{iso} for Si in the T_2O site is −94 ppm and −92 ppm for Si in the T_2m site. These results suggest that the *size* of these clusters are reasonable approximations of the crystalline albite structure and they may see at most a deshielding of 2 to 3 ppm. Unlike crystalline albite, the ^{29}Si-NMR spectrum of albite glass has only one broad peak with a maximum at about −98 ppm (Kohn et al., 1989). However, the maximum lies at the average value of the three peaks of crystalline albite, suggesting that the Si environment does not change dramatically upon vitrification.

Si-O-Al linkages are the most abundant linkages in crystalline albite. Of these linkages in albite, two thirds contain Si[Q^4(3Si,1Al)], while the remaining third contains Si[Q^4(2Si,2Al)]. It is expected that albite glass will also contain primarily these linkages, although additional ones with more or less Al in the neighborhood may exist. Figure 2c shows a cluster model of dry albite glass containing a Si[Q^4(3Si,1Al)]-O-Al[Q^4(4Si,0Al)] linkage. ^{29}Si in this linkage has a δ_{iso} of −98 ppm. This result agrees perfectly with the experimental result for the corresponding T_2O site in crystalline albite. ^{29}Si in a Si[Q^4(2Si,2Al)]-O-Al[Q^4(4Si,0Al)] linkage in a cluster model such as that of Figure 2c, but with only open linkages and more Al in the neighborhood of Si, has a calculated δ_{iso} of −94 ppm. Figure 2d shows a possible configuration containing Si[Q^4(1Si,3Al)]-O-Al[Q^4(4Si,0Al)] in albite glass. The calculated ^{29}Si δ_{iso} for this case is −93 ppm. Thus, it appears that

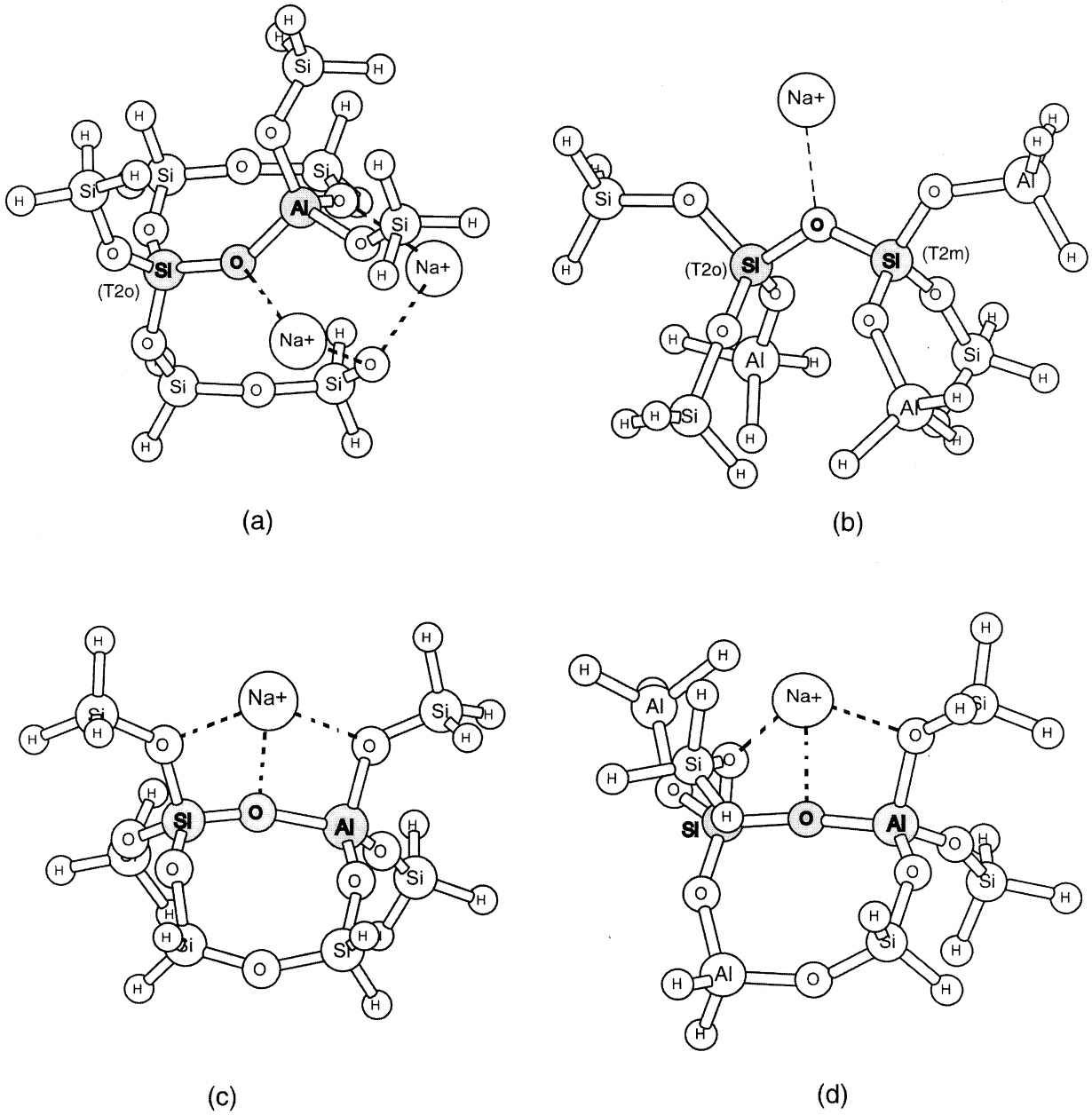

Fig. 2. Cluster models containing (a) a Si[Q^4(3Si,1Al)]$_{T2O}$-O-Al[Q^4(4Si,0Al)] linkage in crystalline low albite; (b) a Si[Q^4(3Si,1Al)]$_{T2O}$-O-Si[Q^4(2Si,2Al)]$_{T2m}$ linkage in crystalline low albite; (c) a Si[Q^4(3Si,1Al)]-O-Al[Q^4(4Si,0Al)] linkage in anhydrous albite glass; (d) a Si[Q^4(1Si,3Al)]-O-Al[Q^4(4Si,0Al)] linkage in anhydrous albite glass. Calculated results for atoms in gray are listed in Table 1.

with more Al in the neighborhood, the ^{29}Si δ_{iso} for this site shifts towards higher frequencies.

Without primarily open linkages, the calculated ^{29}Si δ_{iso} for Si in a Si[Q^4(1Si,3Al)]-O-Al[Q^4(4Si,0Al)] linkage is -104 ppm. This trend is extended by Si in a Si[Q^4(4Si,0Al)]-O-Si[Q^4(4Si,0Al)] linkage which has a calculated δ_{iso} of -111 ppm (using a cluster with three 4-membered rings). Thus, it appears that with more Si in the neighborhood, the ^{29}Si δ_{iso} will shift towards lower frequencies.

These cluster models, however, do not take into account Na^+. Yet, the environment of Na^+ is significantly changed upon the addition of water (e.g., Kohn et al., 1998); thus, there must be strong interactions between Na^+ and water molecules (e.g., Oglesby et al., 2002). Fortunately, because the distance between Na^+ and Si is larger than 3 Å, the effect of the position change of Na^+ (which will move even further from Si) on Si will be rather small. Hence, we can say with confidence, that from a NMR viewpoint, these kinds of cluster model represent the Si environment in albite glass quite well.

Now that the the accuracy of the chosen^{29}Si-NMR calcula-

tion method has been checked, and the requisite size of cluster models considered, we can discuss the implications of the different water dissolution mechanisms for ^{29}Si-NMR properties.

4.1.1. The protonated bridging oxygen model

Figure 3a shows the cluster used to represent a protonated bridging O in an Si[Q^4(3Si,1Al)]-O(H)-Al[Q^4(4Si,0Al)] linkage. Other than for the replacement of the Na^+ with H^+, it is very similar to the model used here for anhydrous albite glass. This linkage also has a chemical environment similar to that of the Si[Q^4(3Si,1Al)]$_{T2O}$-O-Al[Q^4(4Si,0Al)] linkage in the fragment of crystalline albite shown in Figure 2a. It is therefore surprising to obtain a ^{29}Si δ_{iso} of -104 ppm, a value which differs from that for Si in dry glass by 6 ppm and from crystalline albite by 8 ppm. The net increased shielding of Si may perhaps be explained in part by the increase in Si-O bond length from 1.61 to 1.71Å when H replaces Na^+.

Figure 3b shows a model cluster containing a protonated bridging oxygen in the linkage Si[Q^4(2Si,2Al)]-O(H)-Al[Q^4(4Si,0Al)]. This optimized structure has an enlarged bond length of 1.713 Å but otherwise a chemical environment similar to the Si[Q^4(2Si,2Al)]$_{T2m}$ site in crystalline albite. Its calculated ^{29}Si δ_{iso} is -96.4 ppm, compared to the -92.3 ppm experimental value for low albite. It appears, therefore, that protonation of the bridging O of each Si site in albite glass will shift the ^{29}Si δ_{iso} towards lower frequencies by about 5 ppm. Thus, if there are many Al-O(H)-Si species in the glass, we would expect to see a slight shift or the appearance of a shoulder in the hydrous albite glass ^{29}Si-NMR spectrum relative to the dry glass.

We checked further to determine whether additional hydrogen bonding can also affect the Si-NMR properties. A hydrogen bond can also form between H^+ and a dissolved water molecule or nearby oxygen atoms in the network (Fig. 3c). However, it appears that such hydrogen bonding can at most, change the^{29}Si chemical shift by 1 ppm.

Another possible protonated bridging oxygen configuration in hydrous albite glass involves the bridging oxygen of a Si-O-Si linkage (Si-O(H)-Si). The Si-O(H)-Si configuration investigated was similar to that containing the Si[Q^4(3Si,1Al)]$_{T2O}$-O-Si[Q^4(2Al,2Si)]$_{T2m}$ linkage of Figure 2b but with Na^+ replaced by H^+. Si of the Si[Q^4(3Si,1Al)] site yielded a δ_{iso} of -98 ppm; Si of the Si[Q^4(2Al,2Si)] site yielded an δ_{iso} of -95 ppm. This can be compared with the -94 ppm ^{29}Si δ_{iso} obtained for the (H-free) crystalline Si[Q^4(3Si,1Al)]$_{T2O}$ site and -92 ppm obtained for the Si[Q^4(2Al,2Si)]$_{T2m}$ site. Such a Si-O(H)-Si configuration results in greatly enlarged Si-O bond lengths (from 1.61 to 1.80 Å). These long Si-O bonds in a tetrahedral configuration will be very unstable under high temperature conditions and can easily break into two Si[Q^3]-O-H species. Thus, such protonated Si-O-Si linkages are not likely to be very abundant.

4.1.2. The Si[Q^3]-O-H depolymerization model

Farnan et al. (1987) showed that the ^{29}Si chemical shift for Si in Si[Q^3]-O-H will differ from that for Si in Si[Q^4] by about 10 ppm. Kummerlen et al. (1992) found a similar trend for Si in Q^3 species in hydrous sodium silicate glasses. Hence, the formation of any Si[Q^3]-O-H should be reflected in a shift towards the high frequency direction. Although Kohn et al. (1989) concluded that there was no NMR evidence for the presence of Si[Q^3]-O-H species in hydrous alkali aluminosilicate glass, this conclusion deserves further consideration.

There are two readily identifiable Si[Q^3]-O-H forming mechanisms. One involves breaking Al-O-Si linkages; the other, rupture of Si-O-Si linkages. The former mechanism will produce Si[Q^3]-O-H and Al[Q^3]-O-H; the later produces only Si[Q^3]-O-H. Thus, Si-OH linkages in Si[Q^3]-O-H units can have 0, 1, or 2 Al tetrahedra in the next nearest neighborhood (NNN). We evaluated the effects of these different environments using the cluster models of Figure 4.

^{29}Si in Si[Q^3(3Si,0Al)]-O-H linkages produced by rupture of Si[Q^4(4Si, 0Al)]-O-Si[Q^4(4Si, 0Al)] linkages in 4-membered rings (Fig. 4a) upon the dissolution of water, has a calculated δ_{iso} of -101 ppm. This reflects about a 10 ppm shift difference from the ^{29}Si δ_{iso} of Si in the polymerized linkage in anhydrous albite glass (-111 ppm). A simpler model of Si[Q^3(3Si,0Al)]-O-H linkages (Fig. 4b) yields a calculated ^{29}Si δ_{iso} of -96 ppm. The difference between the two models is consistent with previous conclusions that simple clusters will systematically yield results reflecting a deshielded model environment, that is, a shift of the ^{29}Si δ_{iso} towards the high frequency direction by a few ppm. Thus, it is likely that the real value of the δ_{iso} for ^{29}Si is likely to lie between -98 and -101 ppm. The calculated strong shift of the ^{29}Si δ_{iso} towards higher frequencies upon the formation of Si[Q^3(3Si,0Al)]-O-H by rupture of Si[Q^4(4Si, 0Al)]-O-Si[Q^4(4Si, 0Al)] linkages is consistent with the experimental trend of Farnan et al. (1987) and Kummerlen et al. (1992), and suggests that the presence of a significant amount of Si[Q^3(3Si,0Al)]-O-H in hydrous glass should be clearly seen in ^{29}Si-NMR spectra.

Si in Si[Q^3(3Si,0Al)]-O-H linkages produced by rupture of Si[Q^4 (3Si,1Al)]-O-Al[Q^4(4Si,0Al)] linkages (of Fig. 2c) has a ^{29}Si δ_{iso} that differs by about 5 ppm from that of Si in the fully polymerized, unruptured linkage. In contrast, Si in Si[Q^3(2Si,1Al)]-O-H linkages formed by rupture of Si[Q^4 (3Si,1Al)]-O-Si[Q^4(3Si,1Al)] linkages (Fig. 4d) has a calculated isotropic chemical shift difference of about 12 ppm relative to Si in the fully polymerized environment.

It appears that the formation of Si[Q^3]-O-H will causes a shift of ^{29}Si δ_{iso} towards higher frequencies. However, additional H-bonding may be able to reduce the extent of this shift. This possibility was explored using several small clusters (e.g., Fig. 4c). If a water molecule is added to a Si[Q^3(3Si,0Al)]-O-H linkage that was produced by rupture of a Si[Q^4(4Si, 0Al)]-O-Si[Q^4(4Si, 0Al)] linkage, and both the distance to the H atom and the Si-O_H-O_{H2O} are fixed at 1.8 Å, and 140°, respectively, the ^{29}Si δ_{iso} changes from -96 to -98 ppm. (The fixed angle simulates H-bonding arising from linkages beyond the next nearest neighborhood.) If this angle is changed to 170° (in 10° increments), the O of the water molecule moves to a position more directly above the Si-OH bond, while retaining the same H. . .O distance (1.8 Å), and the ^{29}Si δ_{iso} changes from -98 to -100, -102, and finally to -105 ppm. Thus, hydrogen bonding from water molecules or from nearby network oxygen atoms can readily shift the δ_{iso} for ^{29}Si in Si[Q^3]-O-H linkages to lower frequencies by a few ppm, thereby reducing the difference between the ^{29}Si δ_{iso} in the polymerized and the

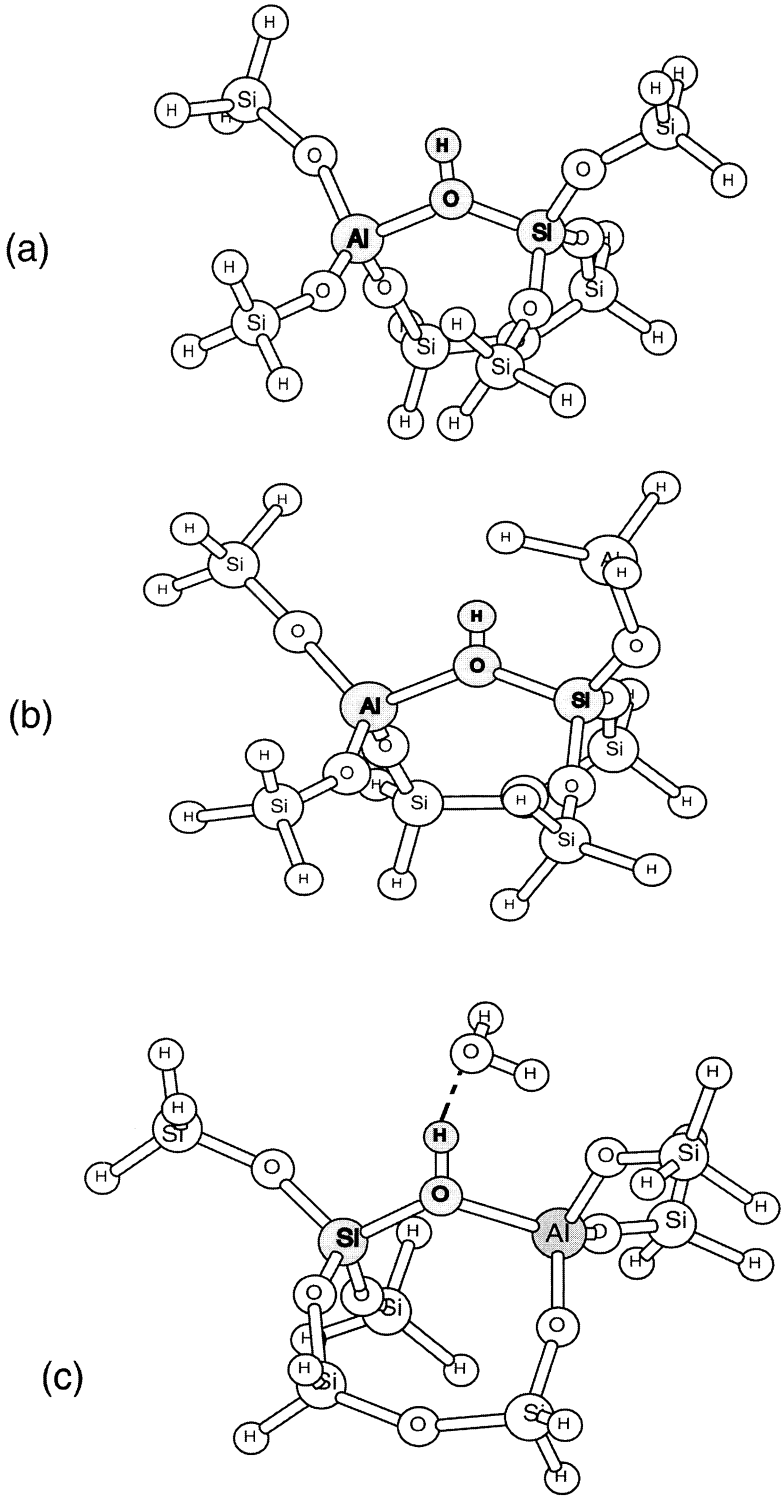

Fig. 3. Cluster models containing (a) a protonated bridging oxygen in the linkage Si[Q^4(3Si,1Al)]-O(H)-Al[Q^4(4Si,0Al)]; (b) a protonated bridging oxygen in the linkage Si[Q^4(2Si,2Al)]-O(H)-Al[Q^4(4Si,0Al)] and (c) additional hydrogen bonding between a water molecule and the linkage Si[Q^4(3Si,1Al)]-O(H)-Al[Q^4(4Si,0Al)]. Calculated results for atoms in gray are listed in Table 1.

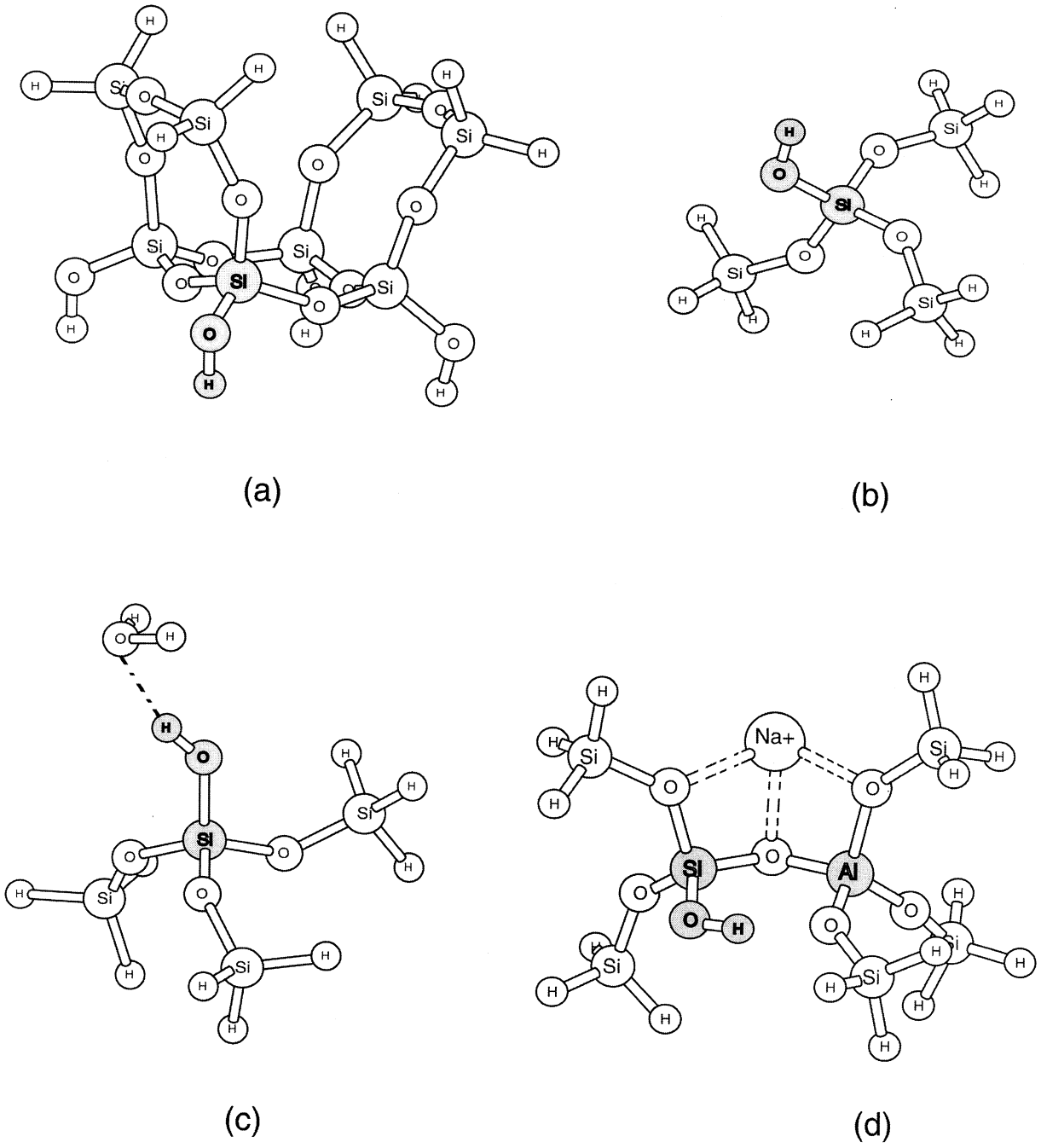

Fig. 4. (a) Cluster model containing the linkages Si[Q^3(3Si,0Al)]-O-H obtained by rupture of Si[Q^4(4Si,0Al)]-O-Si[Q^4(4Si,0Al)] linkages upon water dissolution; (b) simpler cluster model of (a); (c) cluster model containing Si[Q^3(3Si,0Al)]-O-H with additional H-bonding to a water molecule; (d) Si[Q^3(2Si,1Al)]-O-Al[Q^4(4Si,0Al)] linkage in cluster formed by rupture of Si[Q^4(3Si,1Al)]-O-Si[Q^4(3Si,1Al)] linkage. Calculated results for atoms in gray are listed in Table 1.

de-polymerized environments. The extent of this reduction, however, depends upon the H-bonding direction.

4.2. ^{27}Al NMR

The experimental peak maximum of the ^{27}Al resonance in dry albite glass lies at 50.5 ppm for 8.45 T (Kohn et al., 1989) and at 54.8 ppm for 11.7 T (Oestrike et al., 1987). If the quadrupolar coupling constant (C_q) is about 3.5 to 4.0 MHz (i.e., similar to the results of Dirken et al., 1995 who obtained an Al C_q of 3.9 MHz for glass of composition $NaAlSi_{5.3}O_{12.6}$), we estimate the isotropic chemical shift δ_{iso} for ^{27}Al in dry albite glass to be about 60 to 64 ppm. This

value is similar to that of Schmidt et al. (2000), who recorded a value for the δ_{iso} of ^{27}Al of about 58 ppm for a more siliceous glass.

4.2.1. The protonated bridging oxygen model

^{27}Al in a Si[Q^4(3Si,1Al)]-O-Al[Q^4(4Si,0Al)] linkage in the cluster model used for dry albite glass (Fig. 2c), yields a calculated δ_{iso} of 63 ppm using the Hartree-Fock (HF) method and 60 ppm by the B3LYP method. Both values agree well with the experimental data (about 60 ppm). ^{27}Al in the protonated linkage Si[Q^4(3Si,1Al)]-O(H)-Al[Q^4(4Si,0Al)] of Figure 3a in hydrous albite glass yields a δ_{iso} of 64 ppm by the HF and 61 ppm by the B3LYP method; both results are close to the experimental data. Additional hydrogen bonding (Fig. 3c) produces only a minor effect on the ^{27}Al δ_{iso}.

The effect of protonation on the Cq must be carefully considered because of the uncertainty of calculated Cq values, yet its importance when considering quadrupolar nuclei. The Al in Al-O-Si linkages in the anhydrous glass models of Figures 2c andd (with an additional Na^+ cation) yields a reasonable calculated ^{27}Al C_q value of 3.4 MHz. However, the ^{27}Al in the Al-O(H)-Si cluster models of Figure 3a and b yields a C_q value of 13 MHz, suggesting that replacement of Na^+ by H^+ causes a sharp increase in the C_q. Such a dramatic increase in C_q (from $\sim$5 MHz to $-$16 MHz) upon protonation of an Al-O-Si linkage has been seen experimentally in a ZSM-5 zeolite (e.g., Hunger and Horvath, 1995; Grey and Vega, 1995). However, for hydrous glass, this result appears to run counter to known experimental results that suggest that the C_q of ^{27}Al may have a slightly smaller value in hydrous glasses (e.g., Kohn et al., 1989; Sykes et al., 1997) than dry glasses. H-bonding cannot explain the difference between the calculated and observed Cq for ^{27}Al in hydrous glass since H-bonding (e.g., as in Fig. 3c) caused by an additional water molecule will reduce the C_q of Al only slightly; the remainder (about 10MHz) is still very large.

4.2.2. The Al[Q^3]-O-H depolymerization model

The same simple clusters of Figure 4b and c were used to calculate the ^{27}Al NMR properties for Al[Q^3(3Si,0Al)]-O-H linkages with, however, Al as the central atom. Without hydrogen bonding, the calculated ^{27}Al δ_{iso} is around 73 ppm using both the HF and B3LYP levels. With hydrogen bonding, when the O (in H_2O). . .H distance is fixed at 1.8 Å (as an extreme) and the Al-O(H)-O(H_2O) at 150°, the ^{27}Al δ_{iso} is 70 ppm. There is at least a 10 ppm difference between this value and the experimental maximum position. Hence, if there is a significant amount of Al[Q^3]-O-H present in the glass, a shift of the peak maximum or the appearance of a shoulder on the high frequency side of the peak should be observed.

Another interesting issue relates to the C_q value for ^{27}Al in the Al[Q^3]-O-H linkages. All experimental data on hydrous aluminosilicate glasses suggest a decrease in C_q upon hydration. Kohn et al. (1994) and Schmidt et al. (2000) suggested that ^{27}Al in Al[Q^3]-O-H would have a larger C_q than ^{27}Al in a fully polymerized linkage. However, based on their ab initio quantum chemistry calculations, Sykes et al. (1997) concluded that ^{27}Al has a *smaller* C_q in Al[Q^3]-O-H. Our calculated C_q for ^{27}Al in the Al[Q^3(3Si,0Al)]-O-H linkage is 3.4 MHz for Al as the central atom. This is the same as what is calculated for ^{27}Al in a Si[Q^4(3Si,1Al)]-O-Al[Q^4(4Si,0Al)] linkage. If a Na^+ or H_2O water molecule is added to the vicinity of the Al[Q^3(3Si,0Al)]-O-H linkage, the C_q will become a little smaller. Although the uncertainty of the EFG calculation on these small clusters makes it difficult to confidently conclude one way or the other, in most of the cases that we have investigated, the ^{27}Al of the Al[Q^3]-O-H linkages appears to have a smaller C_q value than in any Al[Q^4] environment.

4.3. ^{1}H NMR

Reported experimental ^{1}H-NMR spectra show a major peak centered at 3.5 to 3.8 ppm (e.g., Kohn et al., 1989). Zeng et al. (1999) and Schmidt et al. (2001b) reported in addition, a small sharp peak around 1.3 to 1.5 ppm, which they suggested was caused by Al-OH species.

4.3.1. The protonated bridging oxygen model

The calculated ^1H δ_{iso} for H in the linkage Si[Q^4(3Si,1Al)]-O(H)-Al[Q^4(4Si,0Al)] (Fig. 3a) is 3.7 ppm; this agrees with the major experimental peak very well. With increasing strength of hydrogen bonding, this peak shifts to higher frequencies and may reach more than 10 ppm. Schmidt et al. (2001b) has shown a high-frequency shoulder extending to 10 ppm or more. This protonated bridging oxygen model, however, cannot produce the 1.3 (to 1.5) ppm peak.

4.3.2. The Si [Q^3]-O-H depolymerization model

H in the linkage Si [Q^3]-O-H can have a range of δ_{iso} values that agree with the experimental results well if some hydrogen bonding is also present. For example, if the O (of the H_2O molecule). . .H hydrogen bonding distance is 2.0 Å in the cluster of Figure 4c, the ^1H δ_{iso} is 4.5 ppm; if this distance is 1.8 Å, the ^1H δ_{iso} is 6.3 ppm. With no hydrogen bonding (as may be the case on the surfaces of some fragments), the ^1H δ_{iso} of Si [Q^3]-O-H is 1.5 ppm. This value agrees perfectly with the position of the small peak at 1.3 or 1.5 ppm.

4.3.3. The Al [Q^3]-O-H depolymerization model

The calculated ^1H δ_{iso} for H in the linkage Al [Q^3]-O-H cannot fit the entire range of the major peak (3.3 10 ppm) unless hydrogen bonding is unrealistically strong. Using the cluster showed in Figure 4c but with Al as the central atom, when the hydrogen bond length is 1.8 Å, the calculated ^1H δ_{iso} is 2.6 ppm, which barely extends to the major peak position. When its hydrogen bond length is 1.6 Å, its ^1H δ_{iso} is 5.4 ppm; when its hydrogen bond length is 1.5 Å, its ^1H δ_{iso} is 7.5 ppm. Without hydrogen bonding, H in this linkage will have a ^1H δ_{iso} of –1.4 ppm, which is still far from the 1.3 or 1.5 ppm small experimental peak.

4.4. ^{17}O NMR

^{17}O NMR techniques are becoming increasingly important for clarifying glass structure (e.g., Stebbins et al., 2001). Computational studies have also been carried on ^{17}O (e.g., Tossell, 2001; Xue and Kanzaki, 2000, 2001; Kubicki and Sykes,

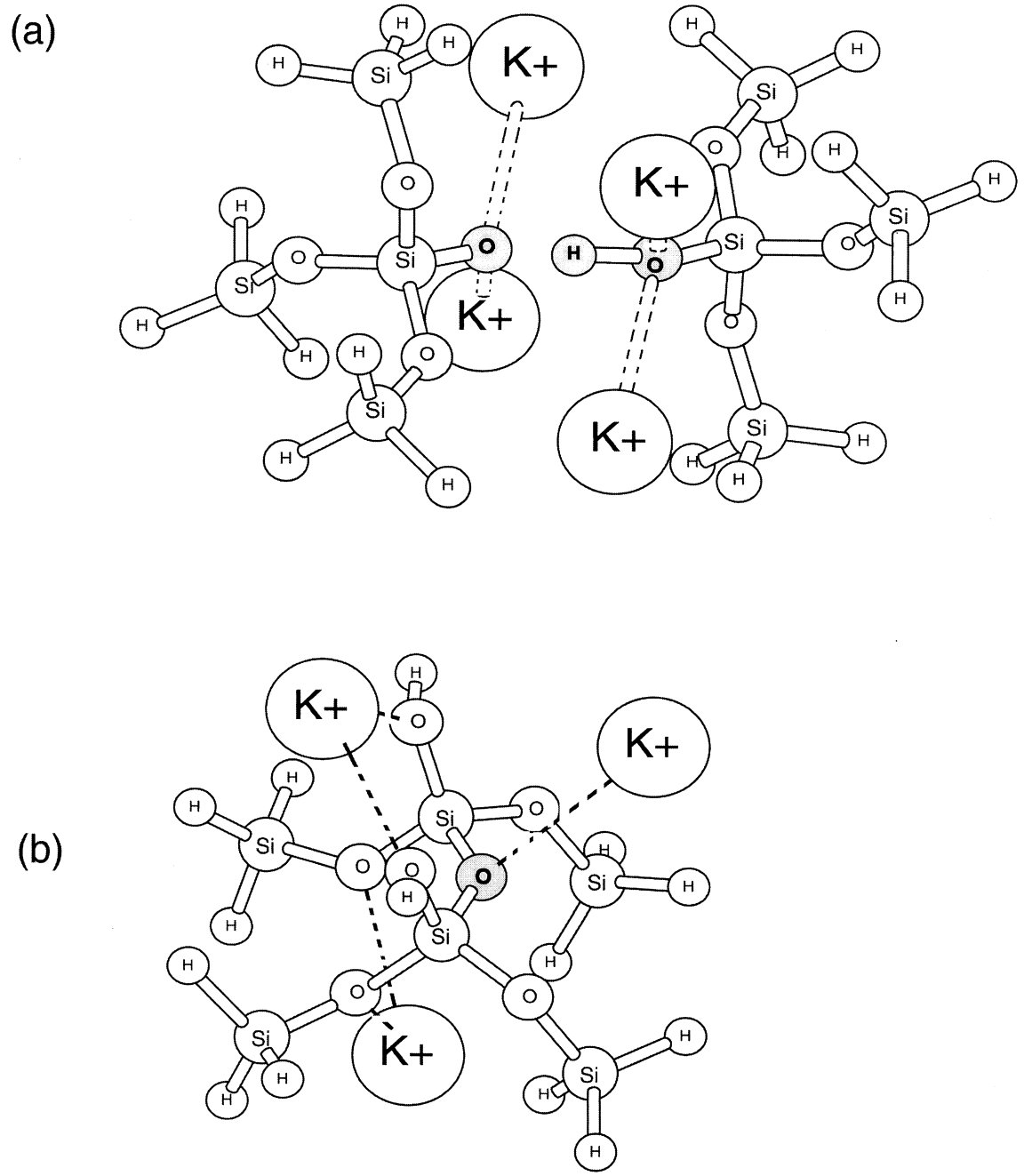

Fig. 5. Cluster models of the (a) NBO and (b) BO environments in crystalline $KHSi_2O_5$ (based X-ray coordinates). Calculated results for atoms in gray are listed in Table 1.

2001). However, there are several complexities involved in such calculations. Even the B3LYP/6–311+G(2df,p) level may not be as accurate for ^{17}O NMR properties as for ^{29}Si, ^{27}Al and ^{1}H. Although the B3LYP/6–311+G(2df,p) level does yield 286 ppm as the shielding value for liquid water, before applying ^{17}O NMR calculations to hydrous albite glasses, however, the accuracy of these calculations must be verified by additional comparisons. Here we compare computational results against known experimental results on crystalline potassium hydrogen disilicate ($KHSi_2O_5$) (Oglesby et al., 2001) and on dry albite glass (Dirken et al., 1997).

Oglesby et al. (2001) showed that crystalline potassium hydrogen disilicate ($KHSi_2O_5$) has two distinct oxygen sites. The bridging oxygen (BO) has a ^{17}O δ_{iso} of 51 ppm and the non-bridging oxygen (NBO) of the Si[Q^3]-O-H linkage, a shift of 60 ppm. Cluster models were built to represent these BO and NBO sites (Fig. 5). The coordinates of all elements other than hydrogen were taken directly from X-ray data (Malinovskii and

Belov, 1979). Since the experimental coordinates for the hydrogen atom are obviously incorrect (i.e., too close to Si), we freely optimized its position using the B3LYP/6–31G* level (with other non-hydrogen elements in fixed positions). Hydrogen atoms added for charge-balance purposes were also optimized at the B3LYP/6–31G* level. The optimized O-H bond length is 1.16 Å and the H atom is shared by another O atom at a distance of 1.28 Å (Fig. 5a); thus, the H atom lies in a double potential well near two O atoms. NMR calculations were then performed on the optimized structure at the B3LYP/6–311+G(2df,p) level.

The NBO (Fig. 5a) has a calculated ^{17}O δ_{iso} of 70 ppm, the BO, a calculated ^{17}O δ_{iso} of 51 ppm (Fig. 5b). The calculated result for the BO is surprising accurate. However, that for the NBO has about a 10 ppm error. This error is most likely caused by the strong H-bonding to the O atoms. The B3LYP/6 to 31G* optimization method appears not good enough to address precisely structural issues of clusters in which strong H-bonding is present. Yet, the O-H bond distance will strongly affect the ^{17}O NMR properties. Since we obtained a very good result for the BO (which is much simpler) it is likely that the level used is suitable for the calculation of ^{17}O NMR properties for clusters without strong H-bonding.

Dirken et al. (1997) showed that the BO of the Al-O-Si linkage in albite glass has a ^{17}O δ_{iso} of 33 ± 1 ppm, while that of the Si-O-Si linkage has a ^{17}O δ_{iso} of 49 ± 1 ppm. Maekawa et al. (1998) obtained a ^{17}O δ_{iso} for the BO of the Al-O-Si linkage of 25 ± 10 ppm and for that of the Si-O-Si site of 40 ± 10 ppm. As is expected for all amorphous materials, there is likely a distribution range of δ_{iso} that includes both sites in the glass. Kubicki and Sykes (2001) based their comparisons on data for albite glass, specifically, a ^{17}O δ_{iso} range of 33 to 43 ppm for the BO in the Al-O-Si linkage and 49 to 58 ppm for the BO of the Si-O-Si linkage. As shown in Figure 2a and b, if a model for crystalline albite based on X-ray coordinates is used, the BO of the Si[Q^4(3Si,1Al)]$_{T2O}$-O-Al[Q^4(4Si,0Al)] linkage (Fig. 2a) has a ^{17}O δ_{iso} of 41 ppm and that of the Si[Q^4(3Si,1Al)]$_{T2O}$-O-Si[Q^4(2Si,2Al)]$_{T2m}$ (Fig. 2b) a ^{17}O δ_{iso} of 53 ppm. There are unfortunately no ^{17}O NMR data on crystalline low albite that can be used for comparison. However, the values are close to the experimental albite glass values and within the distribution range.

The two anhydrous albite glass clusters in Figures 2c and 2d used for modeling a Si[Q^4(3Si,1Al)]-O-Al[Q^4(4Si,0Al)] linkage (Fig. 2c) and a Si[Q^4(1Si,3Al)]-O-Al[Q^4(4Si,0Al)] linkage (Fig. 2d) yield reasonable calculated ^{17}O δ_{iso} for the BO, 41 and 46 ppm, respectively. However, the BO of a Si[Q^4(3Si,1Al)]-O-Si[Q^4(2Si,2Al)] linkage in a cluster similar to Figure 2b, but freely optimized, yields a very unreasonable δ_{iso} ^{17}O value of 65 ppm. This may be caused by unrealistically strong model-induced interactions between the O and the two Na^+ cations. In the real structure, additional linkages beyond the two Na^+ should weaken the interaction. We have checked this by comparisons with a Na^+-free case. Without the two Na^+ atoms, the δ_{iso} ^{17}O of the BO of a Si[Q^4(3Si,1Al)]-O-Si[Q^4(2Si,2Al)] linkage becomes 53 ppm, which is within the 49 to 58 ppm experimental range.

Because there is a rather wide distribution range of the experimental ^{17}O δ_{iso} values, and the fact that the calculation method likely has a several ppm uncertainty, we cannot specifically distinguish different species by using merely their ^{17}O δ_{iso} difference. In recognition of this, only large differences in δ_{iso} of ^{17}O are used here to distinguish species.

4.4.1. The protonated bridging oxygen model

The calculated ^{17}O δ_{iso} of the bridging oxygen of the Si[Q^4(3Si,1Al)]-O(H)-Al[Q^4(4Si,0Al)] (Fig. 3a) linkage is 33 ppm, which is that obtained by Dirken et al. (1997) for the BO of the Al-O-Si linkage in albite glass. Additional hydrogen bonding will shift the ^{17}O δ_{iso} towards the low frequency direction. As shown in Figure 3c, with a 1.75 Å length of the hydrogen bond, the ^{17}O δ_{iso} will change from 33 to 41 ppm, while the ^{1}H δ_{iso} becomes 9.4 ppm.

With more Al in the environment (Fig. 3b) the BO of the Al-O(H)-Si linkage yields a ^{17}O δ_{iso} of 56 ppm, which is outside of the experimental range. This appears to arise from the strong interaction between H^+ near the bridging O site and a terminal H used for charge balance. The ^{1}H δ_{iso} for this linkage is now 11.8 ppm. If such optimization-induced bonding is eliminated, the calculated ^{17}O δ_{iso} is reduced back to within the experimental range.

These results suggest that in general, the bridging oxygen protonation model of Kohn et al. (1989) fits the ^{17}O NMR data quite well. However, they also indicate that ^{17}O NMR properties are sensitive to the surrounding environment (such as the formation of H-bonds) and that agreement or disagreement with the calculated ^{17}O NMR results should not be used as conclusive evidence in support of any model.

It has been speculated that the reason that the protonated O species cannot be seen in the ^{17}O NMR spectra is because the protonated O has a very large C_q. Our calculations indicate that this is not the reason. For example, although the C_q for the BO in the Si[Q^4(3Si,1Al)]-O-Al[Q^4(4Si,0Al)] linkage in anhydrous albite glass (see Fig. 2c) is 4.3 MHz, the C_q of the protonated linkage Si[Q^4(3Si,1Al)]-O(H)-Al[Q^4(4Si,0Al)] (Fig. 3a) is 7.1 MHz. However, with a 1.75 Å H-O bond distance, the C_q of the protonated BO decreases to 2.1 MHz. Thus, with additional H-bonding, the C_q can readily decrease to a value even smaller than that for the non-protonated case.

4.4.2. The Si[Q^3]-O-H depolymerization model

The NBO of the Si[Q^3(3Si,0Al)]-O-H linkage of the clusters of Figures 4a andb yields a calculated ^{17}O δ_{iso} of 17 to 20 ppm. The NBO of the linkage Si[Q^3(2Si,1Al)]-O-H of the cluster of Figure 4d produces a calculated ^{17}O δ_{iso} of ~26 ppm. With additional hydrogen bonding to H, the ^{17}O δ_{iso} for this oxygen shifts to higher frequencies by a few ppm. With hydrogen bonding to O, this ^{17}O δ_{iso} will also shift slightly in the high frequency direction (i.e., by a few ppm). Such H-bonding will therefore shift the ^{17}O δ_{iso} into the experimental range. Because of the rather broad distribution range of ^{17}O δ_{iso} and the uncertainty of the ^{17}O NMR calculation method, we cannot rule out the existence of Si[Q^3]-O-H based on ^{17}O NMR results alone.

4.4.3. The Al[Q^3]-O-H depolymerization model

With no hydrogen bonding, the NBO of the Al[Q^3(3Si,0Al)]-O-H linkage of the cluster of Figure 4b but with Al as the

central atom has a calculated ^{17}O δ_{iso} of about −23 ppm. With additional hydrogen bonding, the ^{17}O δ_{iso} shifts to higher frequencies (e.g., to −17 ppm). For some cases, such as shown by Figure 4c, but with Al as the central atom, the ^{17}O δ_{iso} becomes −2 ppm. Because a large difference remains between the experimental ^{17}O δ_{iso} and that of the NBO in the Al[Q^3(3Si,0Al)]-O-H linkage, we conclude that it is unlikely that this linkage is abundant in hydrous albite glass.

5. CONCLUSIONS

Ab initio NMR computations on a variety of nuclides suggests that calculation of ^{29}Si-NMR resonances are reliable. Computations on ^{1}H and ^{27}Al appear to have only small uncertainties. ^{17}O NMR computational results, however, must be assessed very carefully. Although calculation results for crystalline $KHSi_2O_5$ agree remarkably well with experimental data (for the BO site), ^{17}O NMR properties are very sensitive to the local environment, including the type of atoms within the neighborhood, the number and position of cations, the O-T bond length, and the T-O-T bond angle. Thus, variations in the details of short- to middle-range structural characteristics of glass may strongly affect the ^{17}O NMR properties. The cluster models used here may not be large enough to include all of these factors. On the other hand, the NMR properties of Si, Al and H are not as sensitive and the calculation results are easier to interpret.

From the results of the above calculations, it is clear that a depolymerization model in which the linkages Al[Q^3]-O-H are produced, cannot agree with all of the experimental data. Based on the ^{27}Al NMR calculations, the ^{27}Al δ_{iso} for this linkage will be about 70 to 73 ppm compared with the about 60 ppm experimental value. Meanwhile, its C_q remains unchanged or decreases slightly. If a significant amount of Al[Q^3]-O-H were present, one would expect to see evidence for it through the presence of a shoulder or change in chemical shift. The calculated ^{1}H δ_{iso} without hydrogen bonding is −1.4 ppm; this is far from the major 3.5 to 3.8 ppm peak (which has a left shoulder extending to more than 10 ppm). With very strong hydrogen bonding (e.g., 1.8 Å H. . .O distance), its δ_{iso} is 2.6 ppm, which just barely reaches the major peak. Perhaps the tiny peak can be produced with weak H-bonding; but if so, its δ_{iso} should be continuously distributed and a sharp peak would not be produced. The calculated ^{17}O δ_{iso}, ranges from −23 to −2 ppm, which is far away from the experimental value (roughly 30 to 60 ppm).

The Kohn et al. (1989) model of protonation of Al-O-Si linkages, agrees with most of the experimental data, but this model alone makes it difficult to explain the following observations: (a) ^{29}Si-NMR calculations on hydrous albite glass yield a ^{29}Si δ_{iso} difference of about 5 ppm relative to the anhydrous glass. (b) Calculations based on this model predict an increase in the ^{27}Al C_q. This increase can be moderated but not cancelled out by additional H-bonding caused by H_2O (c) ^{1}H calculations show that for this model the ^{1}H δ_{iso} will not lie around 1.5 ppm where there is a small, but sharp peak in the experimental spectrum.

The Si[Q^3]-O-H depolymerization model, also agrees with most of the data. Especially noteworthy is the prediction of both the small and major peak of the ^{1}H spectrum. But the production of Si[Q^3]-O-H should also induce a clear shift in the high frequency direction. Other factors, such as H-bonding, cannot completely diminish this shift.

Each model discussed here shows some aspect that cannot be reconciled with experimental data. Perhaps both protonation of Al-O-Si linkages and depolymerization of Si-O-Si linkages occur simultaneously upon hydration of albite melt. This combination would explain the presence of the small sharp peak at 1.5 ppm peak in the ^{1}H-NMR spectrum. It could also readily explain the unchanged peak position in the ^{29}Si-NMR spectra upon the addition of water, since the 5 ppm shift of the ^{29}Si δ_{iso} in the low-frequency direction (induced by the protonation of Al-O-Si linkages) can be offset by the shift in the high-frequency direction caused by breakage of Si-O-Si linkages. In addition, this combination can explain the ^{17}O NMR results quite well. This leaves only the question about the increased ^{27}Al C_q produced by the protonation model. Perhaps this can be neglected because of the uncertainty in determining C_q in cluster models containing cations, since these clusters may not be large enough to account for all of the contributions to the EFG.

Such a combined mechanism may have a pathway that starts with protonation of T-O-T bridging oxygens. The lengthened Si-O bonds in the protonated Si-O-Si may then break into Si[Q^3]-O-H units while preserving the protonated Si-O-Al linkages.

Acknowledgments—We thank J. A. Tossell, J. F. Stebbins and Q. Zeng for helpful discussions. We also thank J. B. Parise and J. F. Stebbins for structural data on $KHSi_2O_5$ and J. D. Kubicki and D. G. Sykes for sharing their unpublished data. Three anonymous reviewers have given helpful comments. Support of this work by NSF grant EAR000926 is gratefully acknowledged. MPI publication No. 311.

Associate editor: B. Mysen

REFERENCES

Becke A. D. (1993) A new mixing of Hartree-Fock and local density functional theories. *J. Chem. Phys.* **98,** 1372–1377.

Bull L. M., Bussemer B., Anupold T., Reinhold A., Samoson A., Sauer J., Cheetham A. K., and Dupree R. (2000) A high-resolution O-17 and Si-29 NMR study of zeolite siliceous ferrierite and *ab initio* calculations of NMR parameters. *J. Am. Chem. Soc.* **122,** 4948–4958.

Burnham C. W. (1975) Water and magmas, a mixing model. *Geochim. Cosmochim. Acta* **52,** 2659–2669.

Dingwell D. B. (1998) The glass transition in hydrous granitic melts. *Phys. Earth Planet. Int.* **107,** 1–8.

Dirken P. J., Nachtegaal G. H., and Kentgens A. P. M. (1995) Off-resonance nutation nuclear-magnetic-resonance study of framework aluminosilicate glasses with Li, Na, K, Rb or Cs as charge-balancing cations. *Solid State Nucl. Magn. Res.* **5**(2), 189–200.

Dirken P. J., Kohn S. C., Smith M. E., and van Eck E. R. H. (1997) Complete resolution of Si-O-Si and Si-O-Al fragments in an aluminosilicate glass by ^{17}O multiple quantum magic angle spinning NMR spectroscopy. *Chem. Phys. Lett.* **266,** 568–574.

Ditchfield R. (1974) Self-consistent perturbation theory of diamagnetism I. A gauge-invariant LCAO method for N.M.R. chemical shifts. *Mol. Phys.* **27**(No.4.), 789–807.

Estrin D. A., Paglieri L., Corongiu G., and Clementi E. (1996) Small clusters of water molecules using density functional theory. *J. Phys. Chem.* **100,** 8701–8711.

Farnan I., Kohn S. C., and Dupree R. (1987) A study of the structural role of water in hydrous silica glass using cross-polarisation magic angle spinning NMR. *Geochim. Cosmochim. Acta* **51,** 2869–2873.

Florin AE. and Alei M. Jr. (1967) ^{17}O NMR shifts in H_2 ^{17}O liquid and vapor. *J. Chem. Phys.* **47,** 4268–4269.

Foresman J. B. and Frisch A. E. (1996) *Exploring Chemistry With Electronic Structure Methods*. 2nd Edition. Published by Gaussian, Inc., Pittsburgh, PA 15106 USA.

Frisch M. J., Trucks G. W., Schlegel H. B., Scuseria G. E., Robb M. A., Cheeseman J. R., Zakrzewski V. G., Montgomery J. A., Stratmann R. E., Burant J. C., Dapprich S., Millam J. M., Daniels A. D., Kudin K. N., Strain M. C., Farkas O., Tomasi J., Barone V., Cossi M., Cammi R., Mennucci B., Pomelli C., Adamo C., Clifford S., Ochterski J., Petersson G. A., Ayala P. Y., Cui Q., Morokuma K., Malick D. K., Rabuck A. D., Raghavachari K., Foresman J. B., Cioslowski J., Ortiz J. V., Stefanov B. B., Liu G., Liashenko A., Piskorz P., Komaromi I., Gomperts R., Martin R. L., Fox D. J., Keith T., Al-Laham M. A., Peng C. Y., Nanayakkara A., Gonzalez C., Challacombe M., Gill P. M. W., Johnson B. G., Chen W., Wong M. W., Andres J. L., Head-Gordon M., Replogle E. S., and Pople J. A. (1998) *Gaussian98* Gaussian, Inc., Pittsburgh PA.

Hess K.-U. and Dingwell D. B. (1996) Viscosities of hydrous leucogranitic melts: A non-Arrhenian model. *Am. Min.* **81,** 1297. ¯1300..

Hunger M. and Horvath T. (1995) Multinuclear solid-state NMR study of the local-structure of SiOHAl groups and their interaction with probe-molecules in dehydrated Faujasite and Zeilite ZSM-5. *Ber. Bun. Phys. Chem.* **99,** 1316–1320.

Kirkpatrick R. J. (1988) MAS NMR spectroscopy of minerals and glasses. In *Spectroscopic Methods in Mineralogy and Geology*. (ed. F. C. Hawthorne). *Rev. Mineral* **Vol. 18,** 341–403.

Kohn S. C., Dupree R., and Smith M. E. (1989) A multinuclear magnetic resonance study of the structure of hydrous albite glasses. *Geochim. Cosmochim. Acta* **53,** 2925–2935.

Kohn S. C., Dupree R., and Golan-Mortuza M. (1992) The interaction between water and alumino-silicate magmas. *Chem. Geol.* **96,** 399–409.

Kohn S. C., Smith M. E., and Dupree R. (1994) Comment on "A model for H_2O solubility mechanisms in albite melts from infrared spectroscopy and molecular orbital calculations" by D. Sykes and J. D. Kubicki. *Geochim. Cosmochim. Acta* **58,** 1377–1380.

Kohn S. C., Smith M. E., Dirken P. J., van Eck E. R. H., Kentgens A. P. M., and Dupree R. (1998) Sodium environments in dry and hydrous albite glasses: improved ^{23}Na solid state NMR data and their implications for water dissolution mechanisms. *Geochim. Cosmochim. Acta* **62,** 79–87.

Kubicki J. D., Sykes D. G. (2001). Ab intio calculation of ^{17}O, ^{27}Al and ^{29}Si NMR parameters in hydrous silica and Na-aluminosilicate glasses. Abstact for the 11th annual V.M. Goldschmidt Conference. 3166, pdf.

Kubicki J. D. and Toplis M. J. (2002) Molecular orbital calculations on aluminosilicate tricluster molecules: Implication for the structure of aluminosilicate glasses. *Am. Mineral.* **87,** 668–678.

Kummerlen J., Merwin L. H., Sebald A., and Keppler H. (1992) Structural role of H_2O in sodium-silicate glasses—results from Si-29 and H-1 NMR spectroscopy. *J. Phys. Chem.* **96,** 6405–6410.

Lange R. A. (1994) The effect of H_2O, CO_2 and F on the density and viscosity of silicate melts. In: *Volatiles in Magmas (Reviews in Mineralogy)*, **Vol. 30,** (eds. M. R. Carroll and J. R. Holloway), pp. 331–369. Mineral. Soc. Am., Washington, D.C.

Lee C., Yang W., and Parr R. G. (1988) Development of the Colle-Salvetti correlation-energy formula into a functional of the electron density. *Phys. Rev. B.* **37,** 785–789.

Liu Y. and Nekvasil H. (2001) *Ab initio* studies of possible fluorine-bearing four- and five- coordinated Al species in aluminosilicate glasses. *Am. Mineral.* **86,** 491–497.

Ludwig R. and Weinhold F. (1999) Quantum cluster equilibrium theory of liquids: freezing of QCE/3-21G water to tetrakaidecahedral "Bucky-ice." *J. Chem. Phys.* **110,** 508–515.

Malinovskii Y. A. and Belov N. Y. (1979) Crystal structure of potassium disilicate $KHSi_2O_5$. *Dokolady Akademii Nauk, SSSR.* **246,** 99–103.

Maekawa H., Saito T., and Yokokawa T. (1998) Water in silicate glass: ^{17}O NMR of hydrous silica, albite, and $Na_2Si_4O_9$ glasses. *J. Phys. Chem. B.* **102,** 7523–7529.

Mysen B. O. and Virgo D. (1986) Volatiles in silicate melts at high pressure and temperature. 1. Interaction between OH groups and Si, Al, Ca, Na and H. *Chem. Geol.* **57,** 303–331.

Mysen B. O. and Wheeler K. (2000) Solubility behavior of water in haploandesitic melts at high pressure and high temperature. *Am. Miner.* **85,** 1128–1142.

Nymand TM., Åstrand P., and Mikkelsen KV. (1997) Chemical shifts in liquid water calculated by molecular dynamics simulations and shielding polarizabilities. *J. Phys. Chem. B.* **101,** 4105–4110.

Oestrike R., Yang W. H., Kirkpatrick R. J., Hervig R. L., Navrotsky A., and Montez B. (1987) High-resolution ^{23}Na, ^{27}Al and ^{29}Si NMR spectroscopy of framework aluminosilicate glasses. *Geochim. Cosmochim. Acta* **51,** 2199–2209.

Oglesby J. V. and Stebbins J. F. (2000) Si-29 CPMAS NMR investigations of silanol-group minerals and hydrous aluminosilicate glasses. *Am. Mineral.* **85,** 722–731.

Oglesby J. V., Kroeker S., and Stebbins J. F. (2001) Potassium hydrogen disilicate: A possible model compound for ^{17}O NMR spectra of hydrous silicate glasses. *Am. Miner.* **86,** 341–347.

Oglesby J. V., Zhao P., and Stebbins J. F. (2002) Oxygen sites in hydrous aluminosilicate glasses: The role of Al-O-Al and H_2O. *Geochim. Cosmochim. Acta* **66,** 291–301.

Richet P. and Polian A. (1998) Water as a dense ice-like component in silicate glasses. *Science* **281,** 396–398.

Schmidt B. C., Behrens H., Riemer T., Kappes R., and Dupree R. (2001a) Quantitative determination of water speciation in aluminosilicate glasses: a comparative NMR and IR spectroscopic study. *Chem. Geol.* **174,** 195–208.

Schmidt B. C., Riemer T., Kohn S. C., Holtz F., and Dupree R. (2001b) Structural implications of water dissolution in haplogranitic glasses from NMR spectroscopy: Influence of total water content and mixed alkali effect. *Geochim. Cosmochim. Acta* **65,** 2949–2964.

Schmidt B. C., Riemer T., Kohn S. C., Behrens H., and Dupree R. (2000) Different water solubility mechanisms in hydrous glasses along the Qz-Ab join: Evidence from NMR spectroscopy. *Geochim. Cosmochim. Acta* **64,** 513–526.

Silver L. and Stolper E. (1989) Water in albite glasses. *J. Petrol.* **30,** 667–709.

Stebbins J. F., Oglesby J. V., and Lee S. K. (2001) Oxygen sites in silicate glasses: a new view from oxygen-17 NMR. *Chem. Geol.* **174,** 63–75.

Stolper E. M. (1982) The speciation of water in silicate melts. *Geochim. Cosmochim. Acta* **46,** 2609–2620.

Sykes D. and Kubicki J. D. (1993) A model for H_2O solubility mechanisms in albite melts from infrared spectroscopy and molecular orbital calculations. *Geochim. Cosmochim. Acta* **57,** 1039–1052.

Sykes D. and Kubicki J. D. (1994) Reply to the comment by S. C. Kohn, M. E. Smith and R. Dupree on "A model for H_2O solubility mechanisms in albite melts from infrared spectroscopy and molecular orbital calculations." *Geochim. Cosmochim. Acta* **58,** 1381–1384.

Sykes D., Kubicki J. D., and Farrar T. C. (1997) Molecular orbital calculation of ^{27}Al and ^{29}Si NMR Parameters in Q^3 and Q^4 aluminosilicate molecules and implications for the interpretation of hydrous aluminosilicate glass NMR spectra. *J. Phys. Chem. A.* **101,** 2715–2722.

Taylor M. and Brown G. E. (1979) Structure of mineral glasses.1. Feldspar glasses $NaAlSi_3O_8$, $KAlSi_3O_8$, $CaAl_2Si_2O_8$. *Geochim. Cosmochim. Acta* **43,** 61–75.

Thiessen W. E. and Narten A. H. (1982) Neutron diffraction study of light and heavy water mixtures at 25°C. *J. Chem. Phys.* **77,** 2656–2662.

Tossell J. A. (1999) Quantum mechanical calculation of ^{23}Na NMR shieldings in silicates and aluminosilicates. *Phys. Chem. Minerals* **27,** 70–80.

Tossell J. A. (2001) Calculation of the structural and NMR properties of the tridecameric $AlO_4Al_{12}(OH)_{24}(H_2O)_{12}^{7+}$ polycation. *Geochim. Cosmochim. Acta* **65,** 2549–2553.

Wilson P. J., Amos R. D., and Handy N. C. (1999) Density functional predictions for magnetizabilities and nuclear shielding constants. *Mol. Phys.* **97,** 757–768.

Withers A. C. and Behrens H. (1999) Temperature induced changes in the NIR spectra of hydrous albitic and rhyolitic glasses: implications for hydrous speciation reaction. *Phys. Chem. Minerals* **27,** 119–132.

Xantheas SS. and Dunning TH. Jr. (1993) Ab initio studies of cyclic water clusters $(H_2O)_n$, n=1–6. I. Optimal structures and vibrational spectra. *J. Chem. Phys.* **99,** 8774–8792.

Xu Z., Maekawa H., Oglesby J. V., and Stebbins J. F. (1998) Oxygen speciation in hydrous silicate glasses: an oxygen-17 NMR study. *J. Am. Chem. Soc.* **120,** 9894–9901.

Xue X. and Kanzaki M. (2000) *An ab initio* calculation of ^{17}O and ^{29}Si NMR parameters for SiO_2 polymorphs. *Solid State Nucl. Magn. Reson.* **16,** 245–259.

Xue X. and Kanzaki M. (2001) *Ab initio* calculation of the ^{17}O and ^{1}H NMR parameters for various OH groups: implications to the speciation and dynamics of dissolved water in silicate glasses. *J. Phys. Chem. B.* **105,** 3422–3434.

Zeng Q., Nekvasil H., and Grey C. P. (1999) Proton environments in hydrous aluminosilicate glasses: A H-1 MAS, H-1/Al-27, and H-1/Na-23 TRAPDOR NMR study. *J. Phys. Chem. B.* **103,** 7406–7415.

Zeng Q., Nekvasil H., and Grey C. P. (2000) In support of a depolymerization model for water in sodium aluminosilicate glasses: Information from NMR spectroscopy. *Geochim. Cosmochim. Acta* **64,** 883–896.